Photoinduced Energy Transfer in Linear Guest−Host Chromophores: A Computational Study

Published as part of The Journal of Physical Chemistry virtual special issue "Alexander Boldyrev Festschrift".

L. Alfonso-Hernandez, N. Oldani, S. Athanasopoulos, J. M. Lupton, S. Tretiak, and S. Fernandez-Alberti*

Read Online

ACCESS | Metrics & More | Article Recommendations | Supporting Information
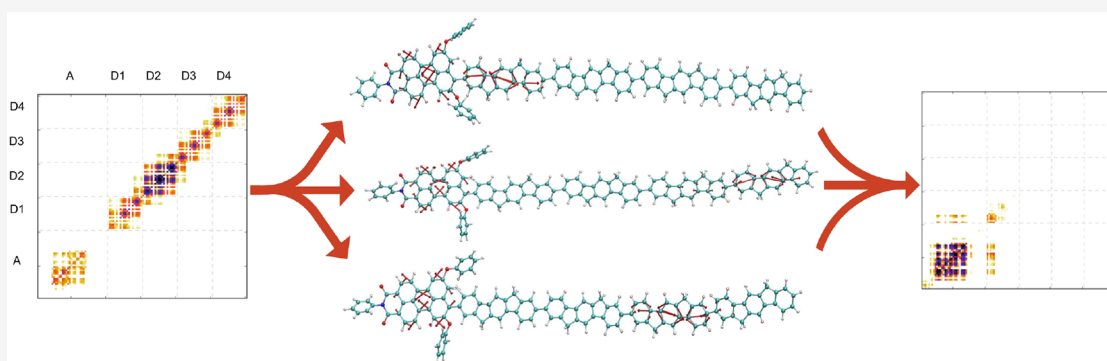
ABSTRACT: Polymer-based guest−host systems represent a promising class of materials for efficient light-emitting diodes. The energy transfer from the polymer host to the guest is the key process in light generation. Therefore, microscopic descriptions of the different mechanisms involved in the energy transfer can contribute to enlighten the basis of the highly efficient light harvesting observed in this kind of materials. Herein, the nature of intramolecular energy transfer in a dye-end-capped conjugated polymer is explored by using atomistic nonadiabatic excited-state molecular dynamics. Linear perylene end-capped (PEC) polyindenofluorenes (PIF), consisting of n (n = 2, 4, and 6) repeat units, i.e., PEC−PIF$_n$ oligomers, are considered as model systems. After photoexcitation at the oligomer absorption maximum, an initial exciton becomes self-trapped on one of the monomer units (donors). Thereafter, an efficient ultrafast through-space energy transfer from this unit to the perylene acceptor takes place. We observe that this energy transfer occurs equally well from any monomer unit on the chain. Effective specific vibronic couplings between each monomer and the acceptor are identified. These oligomer → end-cap energy transfer steps do not match with the rates predicted by Förster-type energy transfer. The through-space and through-bond mechanisms are two distinct channels of energy transfer. The former dominates the overall process, whereas the through-bond energy transfer between indenofluorene monomer units along the oligomer backbone only makes a minor contribution.

I. INTRODUCTION

The photophysical properties of polymer-based guest−host systems have attracted substantial interest since these can serve as models to design bright and efficient light-emitting diodes[1] and photovoltaic devices, and they have potential applications in biophotonics, sensing, imaging, photocatalysis, and photo-dynamic therapy, among others.[2] The principal interest in these materials stems from their chemical versatility propelled by advances in organic synthesis that ensures tunability of the electronic, optical, and mechanical properties.[3] Nowadays, prototype devices can meet realistic specifications for applications.[4,5] Besides this, their manufacturing processes are simple and inexpensive, involving solution processing[6,7] and polymeric film formation.[8] Within these materials, interchain and intrachain energy-transfer processes coexist and parallel their efficiencies to ultimately lead to an effective energy migration[9−13]

A detailed characterization with a variety of spectroscopic techniques helps improvements in polymer design and synthesis. Conventional spectroscopic methods typically provide bulk-averaged values that commonly do not differentiate between inter- and intramolecular energy transfer[9,14,15] smearing the efficiencies of elementary contribution processes. This is even more complicated in the case of heterogeneous
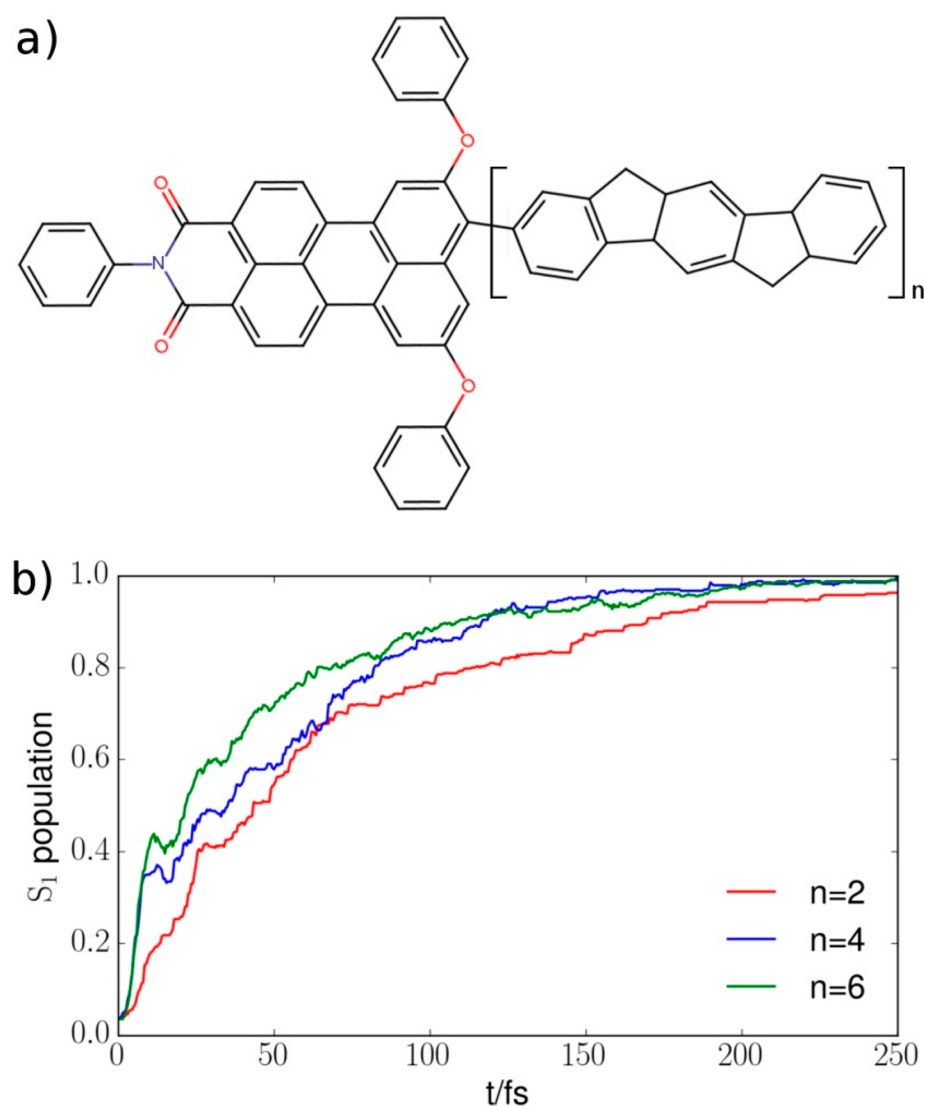
Figure 1. (a) Chemical structure of PEC−PIF$_n$ oligomers. (b) Evolution in time of the average population on S$_1$ obtained from the accumulated fraction of the trajectory ensemble arriving at this state at each given time.

systems such as amorphous polyfluorene films,[16] where conventional spectroscopy and characterization methods are affected by contributions from unwanted green emission bands. Within this context, single-molecule photoluminescence and electroluminescence[17,16] has contributed to unveil the complexity of underpinning photophysical mechanisms.

The energy transfer from the polymer host to the guest chromophore is the key process in light generation. The nonradiative photophysical process involves an excited donor (e.g., a polyfluorene unit) that transfers its excitation energy to an acceptor (e.g., a dye end-cap). The efficiency and rate of the donor-to-acceptor energy transfer is essential for processes required to achieve device functionalities like an efficient internal color conversion by exciton migration[18,19] and promoting chemical sensing,[20] while limiting luminescence quenching due to energy transfer to defects.[12]

Description at atomistic and molecular levels of the different mechanisms involved in the energy transfer in π-conjugated end-capped-oligomers and polymers can contribute to enlighten the basis of the highly efficient light harvesting observed across a variety of such materials.[21] Relative values of donor−acceptor electrostatic and vibronic couplings, structural disorder, and vibrational relaxation rates (cooling) modulate the exciton spatial localization/delocalization among the different chromophores during the energy transfer.[21] Within the so-called weak coupling regime, the rate for donor-to-acceptor energy transfer is well predicted by the Förster Resonant Energy Transfer (FRET) model.[22,23] In these cases, the interchromophore electronic interactions are assumed to be significantly smaller than the vibrational reorganization energy, and therefore, energy migration takes place through sequential incoherent hopping steps between intermediate states that are well localized on the chromophores.[24,25] In contrast, in the strong coupling regime, interchromophore couplings exceed the strength of electron-vibrational interactions, energetic disorder and thermal fluctuations. This leads to delocalized states and the formation of excitonic bands involving multiple chromophores, where the Förster approach is expected to fail.[26] The intermediate coupling regime lies in between these cases, where electronic interactions are comparable to dynamical and static disorder. Here the dynamics involves partially delocalized transient excitons and a careful consideration of all factors affecting the nonequilibrium process (such as coherences) is required.[27]

In this work, the nature of intramolecular energy transfer in a dye-end-capped conjugated polymer is explored by using atomistic nonadiabatic excited-state molecular dynamics modeling. The system under investigation is a simplified linear perylene end-capped (PEC) polyindenofluorenes (PIF), consisting of n (n = 2, 4, and 6) repeat units, i.e., PEC−PIF$_n$ oligomers, whose chemical structure is shown in Figure 1. The double end-capped version of this system has been previously studied by ultrafast spectroscopy combined with quantum-chemical calculations.[14,9,21] These works were able to disentangle the intrachain and interchain energy-migration phenomena. After photoexcitation, light absorbed by the oligomer migrates toward the perylene end-caps. Static and dynamic disorder together with strong nonadiabatic couplings lead to exciton localization over the individual oligomer units and a subsequent incoherent energy migration by exciton hopping. Moreover, energy transfer between oligomer units has been shown to be significantly slower than energy transfer from any oligomer unit to the perylene end-cap. Single molecule spectroscopy measurements performed on this system brought forward a direct analysis of the intramolecular energy transfer process.[28−30] These experiments illustrate the failure of the Förster approach, proving that an efficient energy transfer can occur from the oligomer backbone to the end-cap in the absence of an appreciable spectral overlap between their fluorescence and absorption spectra respectively (a key parameter in the FRET model). In this consideration, the transfer along the oligomer backbone seems to be the rate limiting step for intramolecular energy migration. However, experimentally, energy transfer to the end-cap seems to occur equally well from any segment of the oligomer. The precise nature of the energy transfer process from the PIF to the end-cap still remains unclear. Here, our computational study quantifies various mechanisms involved in the ultrafast energy transfer from the indenofluorene units to the perylene end-cap.

II. METHODS

II.A. Nonadiabatic Excited-State Molecular Dynamics.
Photoinduced dynamics of PEC−PIF$_n$ oligomers have been simulated using the NEXMD package,[31] which has been specifically developed to simulate electronic and vibrational energy relaxation following photoexcitation in large multichromophoric molecular systems. The NEXMD code performs *direct* nonadiabatic excited state molecular dynamics simulations making use of the surface hopping approach[32,33] in combination with "'on the fly'" calculations of excited-state energies, gradients, and nonadiabatic coupling terms analytically using the Collective Electron Oscillator (CEO) approach.[34] The Configuration Interaction Singles (CIS) level in combination with semiempirical model Hamiltonians such as Austin Model 1 (AM1)[35] provide a semiquantitative description of excited state structure in many organic chromophores. The surface hopping method is a hybrid quantum-classical method in which nuclei are propagated classically while the electronic wave function $\psi(t) = \sum_\alpha c_\alpha(t)\phi_\alpha$ is propagated quantum-mechanically using the basis of adiabatic electronic states ϕ_α:

$$i\hbar \dot{c}_{\dot{\alpha}}(t) = c_{\dot{\alpha}}(t)E_{\dot{\alpha}} - i\hbar \sum_\beta c_\beta(t)v \cdot d_{\alpha\beta} \tag{1}$$

where E_α is the energy of the αth electronic adiabatic excited state, $v \cdot d_{\alpha\beta}$ is the nonadiabatic coupling term (NACT$_{\alpha\beta}$), v are

the nuclear velocities associated with nuclear coordinates R, and $d_{\alpha\beta}$ is the nonadiabatic derivative coupling vector (NACR$_{\alpha\beta}$) defined as $d_{\alpha\beta} = \left\langle \phi_\alpha \middle| \frac{\partial \phi_\beta}{\partial R} \right\rangle$.

NEXMD has been successfully applied to simulate the photoinduced dynamics of a broad variety of multichromophoric molecular systems, including donor−acceptor dyads[36] and triads,[37,38] among others.[39] The NEXMD code, license, and documentation may be accessed at https://github.com/lanl/NEXMD. More details related to the NEXMD implementations and parameters can be found elsewhere.[31,39]

II.B. Analyses of Transient Exciton Localization and Migration.
The exciton spatial localization can be monitored throughout the NEXMD simulations by calculating the evolution in time of transition density matrices expressed in atomic orbital (AO) basis: $(\rho^{0\alpha})_{ij} = \langle \phi_\alpha | c_i^\dagger c_j | \phi_0 \rangle$,[40] with ϕ_0 and ϕ_α being the wave functions corresponding to the adiabatic ground and excited states, respectively, and $c_i^\dagger$ and c_j are the respective creation and annihilation operators acting over AO i and j. The diagonal element $(\rho^{0\alpha})_{ii}$ represents the change in the net charge of the electronic density on AO i during a transition from the ground to the excited state α. Consequently, the fraction of $\rho^{0\alpha}$ localized on a specific chromophore unit x is defined as

$$\delta_x^\alpha = (\rho^{0\alpha})_x^{\ 2} = \frac{\sum_{i\in x} (\rho^{0\alpha})_{ii}^{\ 2}}{\sum_i (\rho^{0\alpha})_{ii}^{\ 2}} \tag{2}$$

The extent of the exciton (de)localization within the oligomer can be monitored by defining the monomer participation number[41,42] as

$$\mathrm{PN}(t) = \left[\sum_x (\delta_x^\alpha(t))^2 \right]^{-1} \tag{3}$$

PN(t) ranges from n (the total number of monomers in the oligomer) for a completely delocalized exciton to 1 for an exciton self-trapped on a single monomer unit. It is important to stress that, in order to calculate PN(t), $\rho^{0\alpha}$ needs to be renormalized as $\rho^{0\alpha}/\sum_{x=1,n}\delta_x^\alpha$.

The intraoligomer energy redistribution between indenofluorene monomers as well as the energy transfer between each individual monomer and the end-cap dye can be monitored by using the transition density flux analysis.[43,44] While the method has been presented previously,[43] for the sake of completeness, we briefly outline the basic equations.

At each time interval Δt throughout the NEXMD simulations, the effective change of $\delta_x^\alpha(t)$ denoted as $\Delta\delta_x(t)$ (here, the superindex indicating the state α has been omitted for the sake of simplicity) is calculated by the flow matrix $F(t)$ with null diagonal elements and off-diagonal elements $f_{xy}(t)$ containing the amount of $\delta_x(t)$ transferred between units x and y. The chromophore units are classified as donors (D) if $\Delta\delta_x(t) < 0$ or acceptors (A) if $\Delta\delta x(t) > 0$. By imposing the minimum flow criterion, which assumes that the amount of $\Delta\delta_x(t)$ is a minimum, only the effective $\delta_x(t)$ flow from D to A is taken into account. The total transition density exchanged between the units during time Δt is calculated as

$$\Delta\delta_{total}(t) = \sum_{x \in D} |\Delta\delta_x(t)| = \sum_{y \in A} \Delta\delta_y(t) \tag{4}$$

and elements $f_{yx}(t)$ are evaluated as

$$f_{xy}(t) = -f_{yx}(t)$$

$$= \begin{cases} \dfrac{|\Delta\delta_x(t)||\Delta\delta_y(t)|}{\Delta\delta_{total}(t)} & x \in \mathrm{D}, \, y \in \mathrm{A} \\ 0 & x, \, y \in \mathrm{D} \text{ or } x, \, y \in \mathrm{A} \end{cases} \tag{5}$$

A detailed derivation of eq 5 can be found elsewhere.[43]

II.C. NEXMD Computational Details. The conformational sampling for NEXMD simulations of PEC−PIF$_n$ (n = 2, 4, and 6) was obtained by initially performing an equilibrated ground-state dynamics simulation over 100 ps using the Langevin equation at 500 K with a friction coefficient γ = 20 ps^{-1}. This simulation was used to collect 400 equally spaced configurations for subsequent simulations at 300 K over a duration of 800 ps. After 500 ps of equilibration, initial conditions for NEXMD simulations were collected from each of these simulations. Absorption spectra were obtained from these initial 400 configurations by collecting vertical excitation energies to the 10 lowest excited states and their oscillator strengths. The initial photoexcitations for NEXMD calculations were simulated by a vertical laser excitation to an initial state α with frequency Ω_α selected according to the Franck−Condon window, which is defined as $g_\alpha = f_\alpha \exp[-T^2(E_{laser} - \Omega_\alpha)]$. Here, f_α represents the normalized oscillator strength corresponding to the state α, and E_{laser} is the energy of the simulated laser pulse centered at 425, 439, and 445 nm for n = 2, 4, and 6, respectively. A Gaussian laser pulse $f(t) = \exp\left(\dfrac{-t^2}{2T^2}\right)$, where T = 42.5 fs corresponds to a full width at half-maximum of 100 fs. NEXMD simulations were run at a constant energy for 250 fs. Classical time steps of 0.5 and 0.1 fs were used for the nuclei propagation in ground and excited state trajectories, respectively. In addition, a quantum time step of 0.025 fs was used to propagate the electronic degrees of freedom in nonadiabatic dynamics. Ten excited states were included in the simulations. In addition, NEXMD makes use of specific subroutines to track the identity of states in order to deal with trivial unavoided crossings. The instantaneous decoherence approach, where the electronic wave function is collapsed following an attempted hop (either successful or forbidden), was applied to alleviate problems relating to electronic overcoherence in surface hopping.[45,46]

III. RESULTS AND DISCUSSION

Nonadiabatic excited state molecular dynamics simulations have been performed to model photoinduced intramolecular energy transfer in linear perylene end-capped polyindenofluorenes, PEC−PIF$_n$ oligomers (n = 2, 4, and 6) depicted in Figure 1a. In good agreement with experiments,[28,14] the absorption spectra (see Figure S1) feature the high energy band, associated with the S_2 state spatially localized on the oligomer backbone, and the low energy band is assigned to the perylene absorption at the S_1 state. As expected, the wavelength associated with the oligomer backbone absorption increases with the size n, being 425, 439, and 451 nm for n = 2, 4, and 6, respectively. These energy displacements introduce an important decrease of the S_1−S_2 energy gap with the size of the oligomer.

After photoexcitation at the absorption band associated with the oligomer backbone, mainly dominated by the S_2 state, an ultrafast nonradiative electronic energy relaxation takes place. This relaxation is shown in Figure 1b, where the evolution in
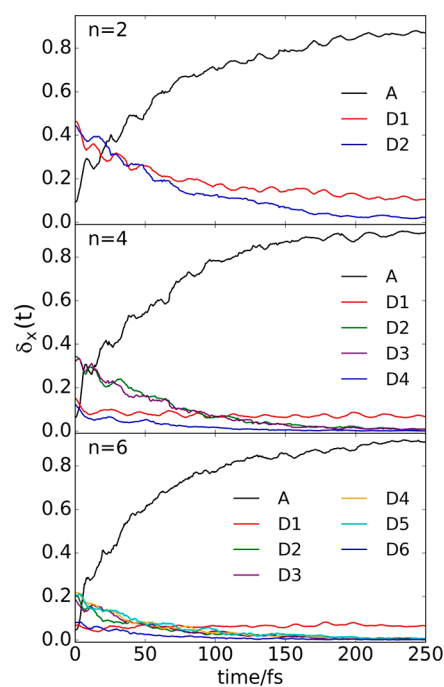
Figure 2. Evolution in time of the fraction of electronic transition density ($\delta_x(t)$) localized on a specific chromophore unit x for PEC−PIF$_n$ oligomers, with n = 2, 4, and 6; x = A (acceptor) corresponds to the perylene acceptor, and x = D1, D2, D3, ..., for each of the indenofluorene monomer units (donor), is numbered in increasing order with respect to their distance to the acceptor A.
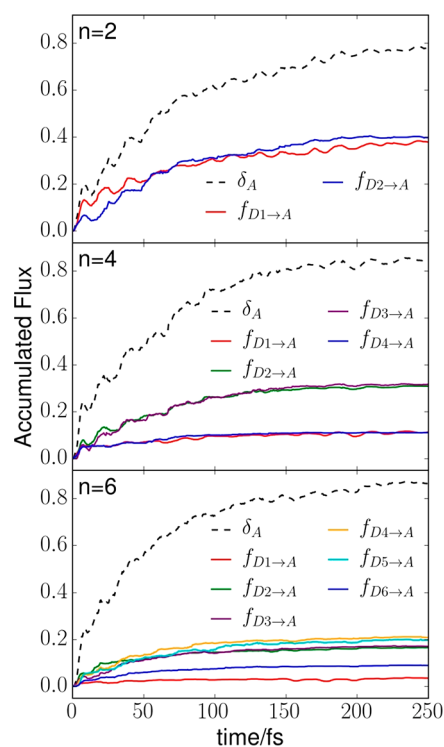
Figure 3. Accumulated transition density flux for each unit (A and Dx (x = 1, ..., n)) in PEC−PIF$_n$ oligomers, with n = 2, 4, and 6.

time of the average population in state S_1 obtained from the accumulated fraction of NEXMD trajectories arriving at this state at each given time is shown. As expected, the S_1 population rapidly increases with time. The rates of population

Table 1. Energy Transfer Rates (fs^{-1}) for the Accumulated Transition Density Fluxes Dx → A from Each of the Indenofluorene Monomers (Dx, (x = 1, ..., n)) to the perylene acceptor A in PEC−PIF$_n$ Oligomers

n	D1	D2	D3	D4	D5	D6
2	0.017	0.014				
4	0.024	0.0175	0.015	0.020		
6	0.035	0.032	0.021	0.021	0.018	0.020

of the S$_1$ state are obtained by fitting to a monoexponential increase function of the form $f(t) = 1 - \exp(-t/\tau)$ where $1/\tau$ represents the rate. Obtained excitation rates ($1/\tau$) are 0.015, 0.020, and 0.025 fs^{-1} for PEC−PIF$_n$ oligomers with n = 2, 4, and 6, respectively. That is, the relaxation rate to the S$_1$ state increases with n. This observation contrasts with previous predicted rates calculated with an improved Förster model.[14]

In order to understand this discrepancy, let us consider different theoretical assumptions that have been used in these previous studies with respect to our simulations. First, FRET models assume a weak donor−acceptor coupling regime, leading to an incoherent energy transfer that involves hopping between well localized chromophores. Calculation of energy transfer rates then proceeds through the evaluation of the overlap between donor emission and acceptor absorption spectra. Additionally, electronic couplings between donor and acceptor states are evaluated at the corresponding optimized geometries. This approach has worked for inter- and intramolecular donor−acceptor energy transfer rates for relatively large donor−acceptor distances (e.g., PEC−PIF$_n$ with many units), achieving a good agreement with ultrafast spectroscopic measurements performed for ensembles of perylene end-capped polyindenofluorenes with an average of
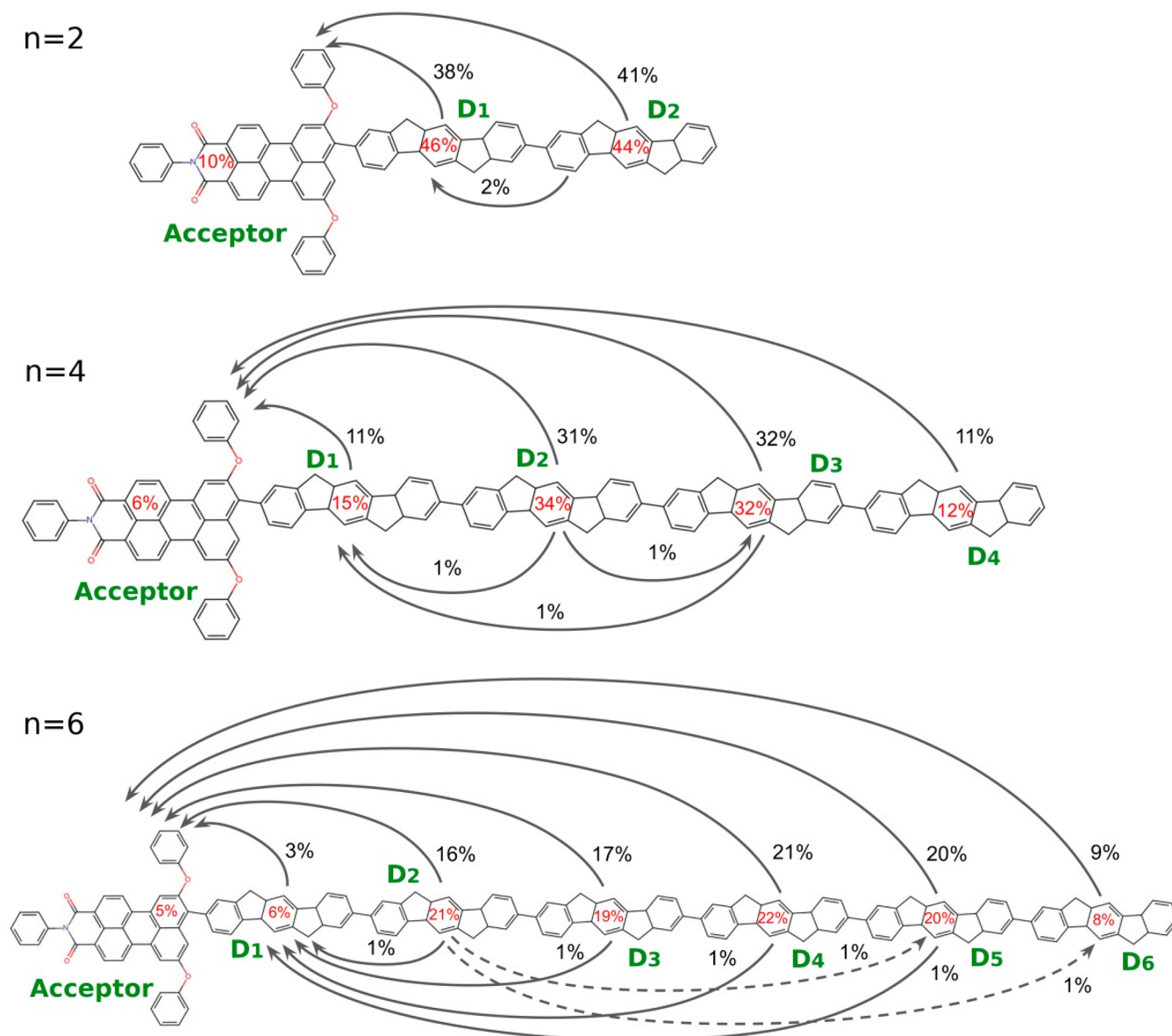
Figure 4. Flowchart summarizing the different pathways contributing to the oligomer-to-end-cap energy transfer in PEC−PIF$_n$ oligomers, with n = 2, 4, and 6. The initial spatial distribution on each unit (A, and Dx (x = 1, ..., n)) is shown in red. Every arrow is labeled with the percentage of transition density transferred through the corresponding channel with respect to the initial excitation. Only channels with contributions ≥1% are shown.
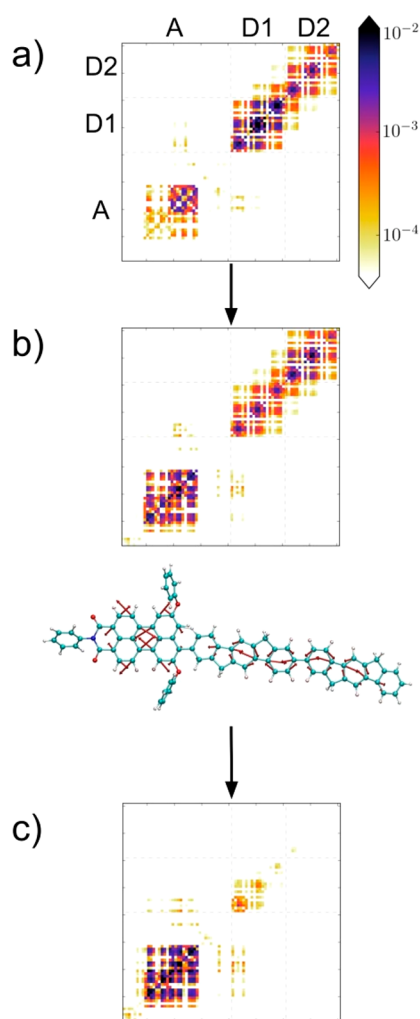
Figure 5. Two-dimensional plots of transition density matrix elements $(\rho^{0\alpha})_{ij}$ in the basis of chromophore atomic orbitals. The plots are shown for representative NEXMD simulations associated with the different energy transfer pathways of PEC−PIF$_2$ (a) at the initial time after photoexcitation, (b) at the moment of the $S_2 \rightarrow S_1$ transition, and (c) at the final time after oligomer $\rightarrow$ end-cap energy transfer is completed. The x and y axes denote the spatial positions of an electron and a hole in the respective atomic orbitals on each unit (A and Dx ($x = 1, ..., n$)). The color coding is shown on the right-hand side. The corresponding nonadiabatic coupling vector at the $S_2 \rightarrow S_1$ transition is also shown.

$n \sim 14$ indenofluorene units. Moreover, due to the uncertainty of the chain length distribution, ranges from $n = 10$ to $n = 100$ have been considered. However, this approximation is expected to fail for smaller covalently bound donor−acceptor systems.[47] In addition to the close proximity of the donor and acceptor, here, conformational disorder due to environmental and thermal fluctuations introduces kinks in the oligomer backbone, breaking the conjugation. Therefore, an initial excitation can be localized on either segment of the oligomer. These segments are strongly coupled with the overlapping absorption and emission profiles, giving rise to multiple energy transfer pathways which coexist. These pathways should be analyzed separately depending on the localization of the initial excitation. Our NEXMD simulations do not assume the weak coupling regime, and they naturally consider an actual case of the intermediate coupling regime, where transient partially delocalized excitons and vibronic coherences can take place

during the relaxation process. This approach can then address the effect of structural, temporal, and energetic disorder during the energy transfer processes. In fact, previous single molecule spectroscopic measurements[28] demonstrate the failure of the Förster theory in these covalently bound molecular aggregates.[48] The experimental data point to the strength and transient character of the oligomer backbone-end-cap coupling responsible for the resulting efficient and fast energy transfer even at room temperature. This contrasts with the less efficient and comparatively slow intramolecular energy transfer involving the exciton hopping along the backbone.

The intraoligomer exciton redistribution emerging after photoexcitation can be analyzed in terms of its fraction of delocalization among the n monomers. Figure S2 depicts the time evolution of the monomer participation number PN(t), averaged over all NEXMD trajectories. Initial values of 1.6, 2.4, and 2.9 for PEC−PIF$_n$ with $n = 2$, 4, and 6, respectively, indicate the initial exciton delocalization across 2−3 indenofluorene monomers. After that, in all cases, PN(t) decreases to ~1.2. That is, during the photoinduced excited state dynamics on the oligomer backbone, before the oligomer $\rightarrow$ end-cap energy transfer takes place, the exciton undergoes an ultrafast self-trapping on one of the monomer units. Such exciton self-trapping in multiple local energetic minima of the backbone involving a single conjugated segment has been previously reported by single molecule spectroscopy.[28]

In order to monitor the effective oligomer-to-end-cap energy transfer process, the time evolution of the fraction of electronic transition density localized on a specific chromophore unit x, ($\delta_x(t)$) has been analyzed, with x being either the perylene acceptor (A), and each of the indenofluorene monomer units is numbered in increasing order (D1, D2, D3, ...) with respect to their distance to the acceptor A. As shown in Figure 2, immediately after photoexcitation to the S_2 state, the molecule experiences an ultrafast excitation transfer between the oligomer units (donors) and the perylene (acceptor). The variations in time of $\delta_A(t)$ are fitted to a monoexponential increase function of the form $f(t) = C - (C - \delta_A(0)) \exp(-t/\tau)$, leading to energy transfer rates ($1/\tau$) of 0.015, 0.018, and 0.022 fs^{-1} for PEC−PIF$_n$ oligomers with $n = 2$, 4, and 6, respectively. In fact, these rates are very close to the values obtained for the population of the S_1 state (Figure 1b), indicating that the $S_2 \rightarrow S_1$ internal conversion process involves the wave function migration from an oligomer to the end-cap underpinning the energy transfer process.

A detailed description of the oligomer-to-end-cap energy transfer can be achieved by analyzing the transition density flux as described in Section II.B. Figure 3 shows the accumulated transition density flux in A and Dx ($x = 1, ..., n$). We observe that the accumulated transition density in A receives population from all Dx units. In fact, all Dx units make only positive contributions to A. Therefore, the end-cap A behaves only as the sole acceptor and never acts as a donor. In order to confirm a unidirectional energy transfer from each Dx to A during $S_2 \rightarrow S_1$ transitions, we monitor the fraction of electronic transition density on A and each Dx monomer (δ_x as a function of delay time, $\tau_{hop} = t - t_{hop}$, relative to the hopping time from S_2 to S_1 on the potential energy surfaces. An average sudden change on δ_x for all x was observed (see Figure S3). This result indicates that all Dx units contribute to their corresponding individual direct D$x \rightarrow$ A exciton transfer.

Table 1 shows the energy transfer rates from each Dx unit to A for each PEC−PIF$_n$ obtained by fitting the transition density
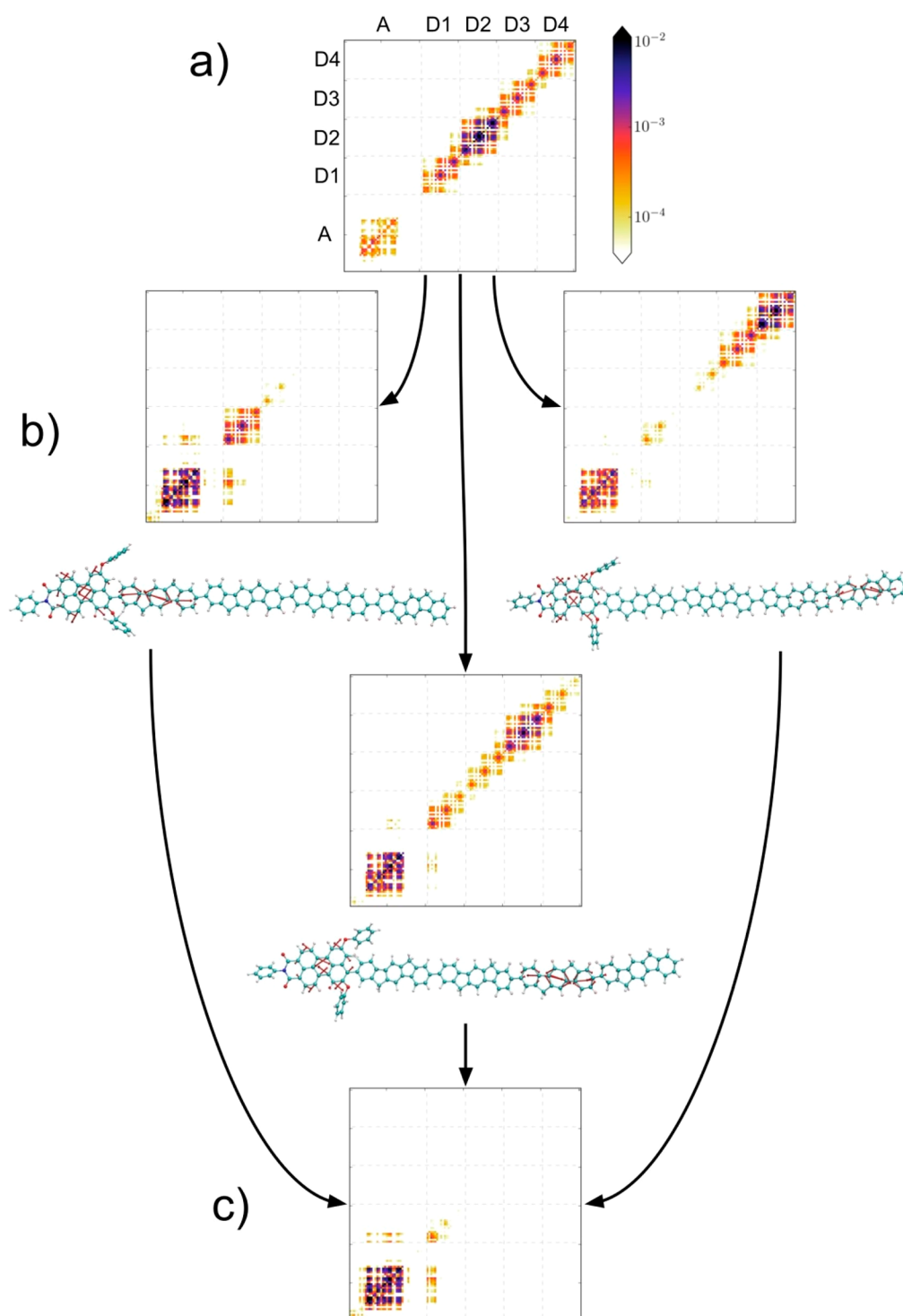
Figure 6. Same as Figure 5 but for PEC−PIF$_4$. In this case, each energy transfer pathway shown in part b corresponds to a different representative trajectory.

flux curves to monoexponential increase function $f(t) = C − C \exp(−t/\tau)$. As expected, we observed that, on average, the rates decrease with the distance between each Dx monomer and A. Moreover, more efficient Dx → A energy transfer is observed for the same values of x in PEC−PIF$_n$ of increasing size n. This reflects a reduction of the S$_1$−S$_2$ energy gap associated with the red shift of the oligomer backbone absorption maximum (S$_2$) with n (see Figure S1).

All pathways that contribute to the oligomer-to-end-cap energy transfer are summarized in Figure 4. An efficient direct Dx → A energy transfer prevails for any Dx monomer according to the transient spatial localization of the self-trapped exciton at the moment of S$_2$ → S$_1$ transition. This agrees well with conclusions from previous single molecule spectroscopy studies[28] that suggested that light harvesting and energy transfer to the end-cap can occur equally well from any segment on the chain. This conclusion was based on the
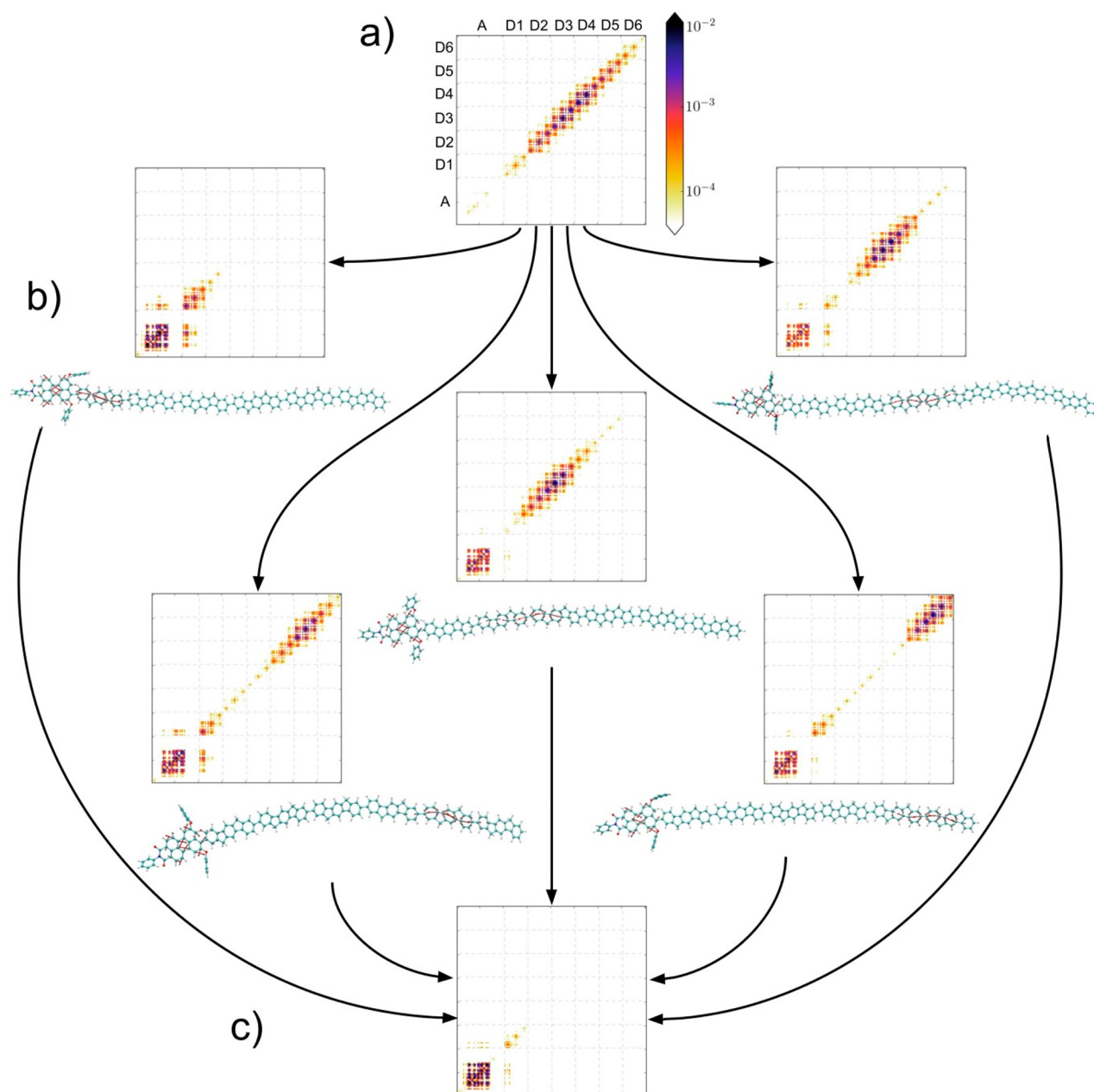
Figure 7. Same as Figure 5 but for PEC−PIF$_6$. Each energy transfer pathway shown in part b corresponds to a different representative trajectory.

similarity in the oligomer backbone excitation polarization anisotropy determined either from the end-cap emission or from the backbone emission. Moreover, minor contributions of inter-Dx energy transfer are also observed in the experiment. However, the data also show the inefficiency of the energy transfer along the oligomer backbone. Actually, the intrachain energy transfer by exciton hopping along the polymer backbone seemingly represents the limiting step in the energy transfer process to the end-cap.[14] In contrast, the end-cap dye and the oligomer backbone form a strongly coupled excited-state complex supporting highly efficient energy transfer to the end-cap. This difference between the intrapolymer vs polymer-to-end-cap energy transfer processes is expected to increase in small oligomers such as those considered in the present study. Therefore, we conclude that the highly efficient and fast oligomer-to-end-cap energy transfer takes place in spite of the lack of exciton exchange between the monomers.

The extent of exciton localization/delocalization during the oligomer-to-end-cap energy transfer can be further analyzed with the entire electronic transition density $\rho^{0\alpha}$ at the moment of the S$_2$ → S$_1$ transition. This is shown in Figures 5−7 that display two-dimensional plots of $\rho^{0\alpha}$ in the basis of the atomic orbitals of the molecule, evaluated at the time of photo-excitation, at the moment of the S$_2$ → S$_1$ transition, and at the final time after the oligomer-to-end-cap energy transfer has concluded. Figure 5 displays the case of PEC−PIF$_2$. Here, the transition density matrix is significantly delocalized across the entire donor (i.e., two indenofluorene monomers) and the end-cap both initially and at the instant of the S$_2$ → S$_1$ transition. Nevertheless, stronger localization on a single monomer is noticeable. Only after the transfer does the excitation become spatially localized on the end-cap. The nuclear motions contributing to electronic coupling during the S$_2$ → S$_1$ transitions can be analyzed by depicting the NACR$_{12}$

vector at that time as shown in Figure 5. We observe that the $NACR_{12}$ motions arise from concerted vibrational dynamics delocalized between the different chromophores. The situation becomes more complicated for the case of $PEC-PIF_4$, where multiple pathways involving different transient exciton self-trapping sites take place (Figure 6). Each energy transfer pathway, taken from a different representative trajectory, involves a different $NACR_{12}$; i.e., differentiation by a spatial localization of S_1 and S_2 electronic states arises when nonadiabatic interactions take place between them.[49] This is even more remarkable for the case of $PEC-PIF_6$ shown in Figure 7. After initial photoexcitation, a pronounced exciton self-trapping on one monomer unit is observed before the $S_2 \rightarrow S_1$ transition occurs. This localization leads to multiple relaxation pathways depending on the number of monomers in the backbone: each unit is able to transiently localize the exciton. As it is observed for $PEC-PIF_4$, each energy transfer pathway pairs with a different vibronic coupling, illustrated by the $NACR_{12}$ vector, spanning the end-cap and the corresponding monomeric indenofluorene unit. This analysis thus clearly distinguishes between the unique energy transfer pathways and the concomitant electronic delocalization and vibronic couplings that make up the integral oligomer-to-end-cap energy transfer events. That is, ultrafast delocalized nuclear motions associated to each differential $NACR_{12}$ vector, shown in Figures 5–7, correspond to the main transient structural distortion observed on each of the associated corresponding trajectories.

IV. CONCLUSIONS

An efficient molecular light-harvesting apparatus should feature concerted and unidirectional energy flow channels. The linear perylene end-capped polyindenofluorenes considered here exemplify such molecular architecture where highly efficient ultrafast oligomer-to-end-cap energy transfer takes place via multiple pathways. Using nonadiabatic excited-state molecular dynamics, we perform detailed analysis of energy transfer dynamics in small $PEC-PIF_n$ systems, consisting of n (n = 2, 4, and 6) repeat units. After photoexcitation at the oligomer backbone absorption band, mainly dominated by the S_2 state, an ultrafast through-space energy transfer takes place to the end-cap state S_1 of lower energy. In spite of the seeming simplicity of this process, there are multiple pathways defined according to the specific transient spatial localization of the exciton during the $S_2 \rightarrow S_1$ transition. Subsequently, a description of this process is nontrivial, and the energy transfer rates do not follow the Förster model predictions, requiring a fully atomistic quantum mechanical description.

In agreement with time-resolved spectroscopic data,[28] we find that the end-cap dye and oligomer backbone form a strongly coupled excited-state complex with highly efficient energy transfer from any of the individual oligomer units. This coupling represents a different scenario compared to the energy transfer in large end-cap-polymers with larger interchromophore distances. Here, in relatively small $PEC-PIF_n$s, the highly efficient and fast through-space oligomer-to-end-cap energy transfer steps are mediated by a transient exciton self-trapping on one of the monomer units and take place to the detriment of exciton exchange between the monomers. As a result, the oligomer-to-end-cap energy transfer occurs equally well from any monomer unit, involving different directions of vibronic coupling. The larger the oligomer, the more pronounced is the exciton transient self-trapping in one

of the monomer units before the $S_2 \rightarrow S_1$ transition. The intermonomer through-bond energy transfer along the oligomer backbone only contributes as a minor energy transfer channel. In the limit of large polymers, the vibronic coupling between each specific monomer and the end-cap is expected to decrease, and therefore, the through-bond intermonomer exciton exchange should become the rate-limiting step for the light harvesting in these systems.[24,50] Altogether, our computational analysis illustrates the complexity of energy transfer processes in light harvesting function performed by assemblies of organic chromophores operating in the intermediate-strength coupling regime. Complementary experimental[28] and quantum-chemical investigations provide deep insights and yield useful design principles to be used in the future synthetic and fabrication efforts.

■ ASSOCIATED CONTENT

ⓈI Supporting Information

The Supporting Information is available free of charge at https://pubs.acs.org/doi/10.1021/acs.jpca.1c02644.

Figure S1, simulated absorption spectra of $PEC-PIF_n$ oligomers with n = (a) 2, (b) 4, and (c) 6, showing the contributions from the 10 lowest individual excited states; Figure S2, evolution in time of the monomer participation number $PN(t)$, averaged over all NEXMD simulations, for $PEC-PIF_n$ oligomers with n = (a) 2, (b) 4, and (c) 6; and Figure S3, fraction of electronic transition density (δ_x on A and each Dx monomer in $PEC-PIF_n$ oligomers with n = (a) 2, (b) 4, and (c) 6 as a function of delay time, $\tau_{hop} = t - t_{hop}$, relative to the hopping time from S_2 to S_1 on the potential energy surface (PDF)

■ AUTHOR INFORMATION

Corresponding Author

S. Fernandez-Alberti − *Departamento de Ciencia y Tecnologia, Universidad Nacional de Quilmes/CONICET, B1876BXD Bernal, Argentina;* ⓞ orcid.org/0000-0002-0916-5069; Email: sfalberti@gmail.com

Authors

L. Alfonso-Hernandez − *Departamento de Ciencia y Tecnologia, Universidad Nacional de Quilmes/CONICET, B1876BXD Bernal, Argentina*

N. Oldani − *Departamento de Ciencia y Tecnologia, Universidad Nacional de Quilmes/CONICET, B1876BXD Bernal, Argentina*

S. Athanasopoulos − *Departamento de Física, Universidad Carlos III de Madrid, 28911 Leganés, Madrid, Spain;* ⓞ orcid.org/0000-0003-0753-2643

J. M. Lupton − *Institut für Angewandte und Experimentelle Physik, Universität Regensburg, 93053 Regensburg, Germany*

S. Tretiak − *Theoretical Division, Center for Nonlinear Studies (CNLS), and Center for Integrated Nanotechnologies (CINT), Los Alamos National Laboratory, Los Alamos, New Mexico 87545, United States;* ⓞ orcid.org/0000-0001-5547-3647

Complete contact information is available at:
https://pubs.acs.org/10.1021/acs.jpca.1c02644

Notes

The authors declare no competing financial interest.

The Nonadiabatic EXcited state Molecular Dynamics (NEXMD) Program code, license, and documentation may be accessed at https://github.com/lanl/NEXMD.

REFERENCES

(1) Friend, R. H.; Gymer, R. W.; Holmes, A. B.; Burroughes, J. H.; Marks, R. N.; Taliani, C.; Bradley, D. D. C.; dos Santos, D. A.; Brédas, J. L.; Logdlund, M.; et al. Electroluminescence in Conjugated Polymers. *Nature* 1999, *397* (6715), 121−128.

(2) Tuncel, D. π-Conjugated Nanostructured Materials: Preparation, Properties and Photonic Applications. *Nanoscale Adv.* 2019, *1* (1), 19−33.

(3) Root, S. E.; Savagatrup, S.; Printz, A. D.; Rodriquez, D.; Lipomi, D. J. Mechanical Properties of Organic Semiconductors for Stretchable, Highly Flexible, and Mechanically Robust Electronics. *Chem. Rev.* 2017, *117* (9), 6467−6499.

(4) Nomura, K. Well-Defined End-Functionalized Conjugated Polymers/Oligomers Exhibiting Unique Emission Properties through the End Groups: The Exclusive Synthesis by Combined Olefin Metathesis with Wittig-Type Coupling. *Macromol. Mater. Eng.* 2019, *304* (9), 1900307.

(5) Jana, B.; Bhattacharyya, S.; Patra, A. Perspective of Dye-Encapsulated Conjugated Polymer Nanoparticles for Potential Applications. *Bull. Mater. Sci.* 2018, *41* (5), 122.

(6) Müller, C. D.; Falcou, A.; Reckefuss, N.; Rojahn, M.; Wiederhirn, V.; Rudati, P.; Frohne, H.; Nuyken, O.; Becker, H.; Meerholz, K. Multi-Colour Organic Light-Emitting Displays by Solution Processing. *Nature* 2003, *421* (6925), 829−833.

(7) Guo, F.; Karl, A.; Xue, Q.-F.; Tam, K. C.; Forberich, K.; Brabec, C. J. The Fabrication of Color-Tunable Organic Light-Emitting Diode Displays via Solution Processing. *Light: Sci. Appl.* 2017, *6* (11), No. e17094.

(8) Felton, L. A. Mechanisms of Polymeric Film Formation. *Int. J. Pharm.* 2013, *457* (2), 423−427.

(9) Beljonne, D.; Pourtois, G.; Silva, C.; Hennebicq, E.; Herz, L. M.; Friend, R. H.; Scholes, G. D.; Setayesh, S.; Müllen, K.; Brédas, J. L. Interchain vs. Intrachain Energy Transfer in Acceptor-Capped Conjugated Polymers. *Proc. Natl. Acad. Sci. U. S. A.* 2002, *99* (17), 10982−10987.

(10) Ryno, S. M.; Risko, C. Deconstructing the Behavior of Donor-Acceptor Copolymers in Solution & the Melt: The Case of PTB7. *Phys. Chem. Chem. Phys.* 2019, *21* (15), 7802−7813.

(11) Bolis, S.; Pasini, M.; Virgili, T. Ultrafast Study of Inter- and Intrachain Energy Transfer in a Core-Polymer. *J. Polym. Sci., Part B: Polym. Phys.* 2018, *56* (13), 965−969.

(12) Athanasopoulos, S.; Hennebicq, E.; Beljonne, D.; Walker, A. B. *J. Phys. Chem. C* 2008, *112*, 11532−11538.

(13) Papadopoulos, T.; Muccioli, L.; Athanasopoulos, S.; Walker, A. B.; Zannoni, C.; Beljonne, D. Does Supramolecular Ordering Influence Exciton Transport in Conjugated Systems? Insight from Atomistic Simulations. *Chem. Sci.* 2011, *2*, 1025.

(14) Hennebicq, E.; Pourtois, G.; Scholes, G. D.; Herz, L. M.; Russell, D. M.; Silva, C.; Setayesh, S.; Grimsdale, A. C.; Müllen, K.; Brédas, J. L.; Beljonne, D. Exciton Migration in Rigid-Rod Conjugated Polymers: An Improved Förster Model. *J. Am. Chem. Soc.* 2005, *127* (13), 4744−4762.

(15) Nguyen, T. Q.; Wu, J.; Doan, V.; Schwartz, B. J.; Tolbert, S. H. Control of Energy Transfer in Oriented Conjugated Polymer-Mesoporous Silica Composites. *Science* 2000, *288* (5466), 652−656.

(16) Honmou, Y.; Hirata, S.; Komiyama, H.; Hiyoshi, J.; Kawauchi, S.; Iyoda, T.; Vacha, M. Single-Molecule Electroluminescence and Photoluminescence of Polyfluorene Unveils the Photophysics behind the Green Emission Band. *Nat. Commun.* 2014, *5*, 4666.

(17) Mitschke, U.; Bäuerle, P. The Electroluminescence of Organic Materials. *J. Mater. Chem.* 2000, *10* (7), 1471−1507.

(18) Halls, J. J. M.; Walsh, C. A.; Greenham, N. C.; Marseglia, E. A.; Friend, R. H.; Moratti, S. C.; Holmes, A. B. Efficient Photodiodes from Interpenetrating Polymer Networks. *Nature* 1995, *376* (6540), 498−500.

(19) Yu, G.; Gao, J.; Hummelen, J. C.; Wudl, F.; Heeger, A. J. Polymer Photovoltaic Cells: Enhanced Efficiencies via a Network of Internal Donor-Acceptor Heterojunctions. *Science* 1995, *270*, 1789−1791.

(20) McQuade, D. T.; Pullen, A. E.; Swager, T. M. Conjugated Polymer-Based Chemical Sensors. *Chem. Rev.* 2000, *100* (7), 2537−2574.

(21) Brédas, J. L.; Beljonne, D.; Coropceanu, V.; Cornil, J. Charge-Transfer and Energy-Transfer Processes in π-Conjugated Oligomers and Polymers: A Molecular Picture. *Chem. Rev.* 2004, *104* (11), 4971−5003.

(22) Förster. Intermolecular Energy Migration and Fluorescence. *Ann. Phys.* 1948, *437* (1-2), 55−75.

(23) May, V.; Kühn, O. *Charge and Energy Transfer Dynamics in Molecular Systems*, 3rd ed.; Wiley-VCH Verlag GmbH & Co. KGaA: 2011.

(24) Athanasopoulos, S.; Emelianova, E. V.; Walker, A. B.; Beljonne, D. Exciton Diffusion in Energetically Disordered Organic Materials. *Phys. Rev. B: Condens. Matter Mater. Phys.* 2009, *80*, 195209.

(25) Ansari-Rad, M.; Athanasopoulos, S. Theoretical Study of Equilibrium and Nonequilibrium Exciton Dynamics in Disordered Semiconductors. *Phys. Rev. B: Condens. Matter Mater. Phys.* 2018, *98*, 085204.

(26) Beljonne, D.; Curutchet, C.; Scholes, G. D.; Silbey, R. J. *J. Phys. Chem. B* 2009, *113* (19), 6583.

(27) Kimura, A.; Kakitani, T. Theory of Excitation Energy Transfer in the Intermediate Coupling Case of Clusters. *J. Phys. Chem. B* 2003, *107* (51), 14486−14499.

(28) Becker, K.; Lupton, J. M. *J. Am. Chem. Soc.* 2006, *128* (17), 6468−6479.

(29) Walter, M. J.; Lupton, J. M. Unraveling the Inhomogeneously Broadened Absorption Spectrum of Conjugated Polymers by Single-Molecule Light-Harvesting Action Spectroscopy. *Phys. Rev. Lett.* 2009, *103* (16), 9−12.

(30) Walter, M. J.; Borys, N. J.; van Schooten, K.; Lupton, J. M. Light-Harvesting Action Spectroscopy of Single Conjugated Polymer Nanowires. *Nano Lett.* 2008, *8*, 3330.

(31) Malone, W.; Nebgen, B.; White, A.; Zhang, Y.; Song, H.; Bjorgaard, J.; Sifain, A.; Rodriguez-Hernandez, B.; Freixas, V.; Fernandez-Alberti, S.; et al. NEXMD Software Package for Non-Adiabatic Excited State Molecular Dynamics Simulations. *J. Chem. Theory Comput.* 2020, *16*, 5771−5783.

(32) Tully, J. C. Molecular Dynamics with Electronic Transitions. *J. Chem. Phys.* 1990, *93*, 1061−1071.

(33) Hammes-Schiffer, S.; Tully, J. C. Proton Transfer in Solution: Molecular Dynamics with Quantum Transitions. *J. Chem. Phys.* 1994, *101* (6), 4657−4667.

(34) Mukamel, S.; Tretiak, S.; Wagersreiter, T.; Chernyak, V. Electronic Coherence and Collective Optical Excitations of Conjugated Molecules. *Science* 1997, *277* (5327), 781−787.

(35) Dewar, M. J. S.; Zoebisch, E. G.; Healy, E. F.; Stewart, J. J. P. The Development and Use of Quantum-Mechanical Molecular-Models.76.AM1 - A New General Purpose Quantum-Mechanical Molecular-Model. *J. Am. Chem. Soc.* **1985**, *107*, 3902−3909.

(36) Athanasopoulos, S.; Alfonso Hernandez, L.; Beljonne, D.; Fernandez-Alberti, S.; Tretiak, S. Ultrafast Non-Förster Intramolecular Donor-Acceptor Excitation Energy Transfer. *J. Phys. Chem. Lett.* **2017**, *8* (7), 1688−1694.

(37) Freixas, V. M.; Nelson, T.; Ondarse-Alvarez, D.; Nijjar, P.; Mikhailovsky, A.; Zhou, C.; Fernandez-Alberti, S.; Bazan, G. C.; Tretiak, S. Experimental and Theoretical Study of Energy Transfer in a Chromophore Triad: What Makes Modeling Dynamics Successful? *J. Chem. Phys.* **2020**, *153*, 244114.

(38) Oldani, N.; Tretiak, S.; Bazan, G.; Fernandez-Alberti, S. Modeling of Internal Conversion in Photoexcited Conjugated Molecular Donors Used in Organic Photovoltaics. *Energy Environ. Sci.* **2014**, *7* (3), 1175.

(39) Nelson, T. R.; White, A. J.; Bjorgaard, J. A.; Sifain, A. E.; Zhang, Y.; Nebgen, B.; Fernandez-Alberti, S.; Mozyrsky, D.; Roitberg, A. E.; Tretiak, S. Non-Adiabatic Excited-State Molecular Dynamics: Theory and Applications for Modeling Photophysics in Extended Molecular Materials. *Chem. Rev.* **2020**, *120* (4), 2215−2287.

(40) Tretiak, S.; Isborn, C. M.; Niklasson, A. M. N.; Challacombe, M. Representation Independent Algorithms for Molecular Response Calculations in Time-Dependent Self-Consistent Field Theories. *J. Chem. Phys.* **2009**, *130*, 054111−054127.

(41) Bell, R. J.; Dean, P.; Hibbins-Butler, D. C. Localization of Normal Modes i n Vitreous Silica, Germania and Beryllium Fluoride. *J. Phys. C: Solid State Phys.* **1970**, *3*, 2111−2118.

(42) Taraskin, S. N.; Elliott, S. R. Anharmonicity and Localization of Atomic Vibrations in Vitreous Silica. *Phys. Rev. B: Condens. Matter Mater. Phys.* **1999**, *59* (13), 8572−8585.

(43) Alfonso Hernandez, L.; Nelson, T.; Gelin, M. F.; Lupton, J. M.; Tretiak, S.; Fernandez-Alberti, S. Interference of Interchromophoric Energy-Transfer Pathways in π-Conjugated Macrocycles. *J. Phys. Chem. Lett.* **2016**, *7* (23), 4936−4944.

(44) Soler, M. A.; Bastida, A.; Farag, M. H.; Zúñiga, J.; Requena, A. A Method for Analyzing the Vibrational Energy Flow in Biomolecules in Solution. *J. Chem. Phys.* **2011**, *135* (20), 204106.

(45) Fernandez-Alberti, S.; Roitberg, A. E.; Nelson, T.; Tretiak, S. Identification of Unavoided Crossings in Nonadiabatic Photoexcited Dynamics Involving Multiple Electronic States in Polyatomic Conjugated Molecules. *J. Chem. Phys.* **2012**, *137* (1), 014512.

(46) Nelson, T.; Fernandez-Alberti, S.; Roitberg, A. E.; Tretiak, S. Nonadiabatic Excited-State Molecular Dynamics: Treatment of Electronic Decoherence. *J. Chem. Phys.* **2013**, *138*, 224111.

(47) Nelson, T.; Fernandez-Alberti, S.; Roitberg, A. E.; Tretiak, S. Conformational Disorder in Energy Transfer: Beyond Forster Theory. *Phys. Chem. Chem. Phys.* **2013**, *15* (23), 9245−9256.

(48) Becker, K.; Lupton, J. M.; Feldmann, J.; Setayesh, S.; Grimsdale, A. C.; Müllen, K. Efficient Intramolecular Energy Transfer in Single Endcapped Conjugated Polymer Molecules in the Absence of Appreciable Spectral Overlap. *J. Am. Chem. Soc.* **2006**, *128*, 680−681.

(49) Soler, M.; Roitberg, A.; Nelson, T.; Tretiak, S.; Fernandez-Alberti, S. Analysis of State-Specific Vibrations Coupled to the Unidirectional Energy Transfer in Conjugated Dendrimers. *J. Phys. Chem. A* **2012**, *116* (40), 9802−9810.

(50) Athanasopoulos, S.; Hoffmann, S. T.; Bässler, H.; Köhler, A.; Beljonne, D. To Hop or Not to Hop? Understanding the Temperature Dependence of Spectral Diffusion in Organic Semiconductors. *J. Phys. Chem. Lett.* **2013**, *4*, 1694.